

DNA–carbon nano onion aggregate: triangle, hexagon, six-petal flower to dead-end network

Dipak Gorakh Babar¹ · Bholanath Pakhira^{2,3} · Sabyasachi Sarkar³ 

Received: 28 March 2017 / Accepted: 11 May 2017 / Published online: 17 May 2017
© The Author(s) 2017. This article is an open access publication

Abstract The interaction between calf-thymus (CT) dsDNA and water soluble carbon nano onion (wsCNO) in water follows denaturation of dsDNA (double stranded) to ssDNA (single stranded) as monitored by optical spectroscopy. The ssDNA concomitantly wraps the spiky surface of wsCNO to create triangular aggregate as the building block as observed by time-dependent SEM images. These triangles further aggregate leading to six-petal flower arrangement via hexagon and finally reach a dead end network as imaged by SEM and optical fluorescence microscopy. The dead-end network aggregate lost the intrinsic optical property of DNA suggesting complete loss of its activity.

Keywords Calf thymus DNA · wsCNO · Self-assembly · Six-petal flower aggregate · Dead-end network

Introduction

Several short single-stranded (ss) DNA interact with a long single-stranded (ss) DNA to generate different shapes such like squares, triangles, and five-pointed stars.

Such scaffolded DNA origami is driven by the creation of novel biomaterials for analytical and therapeutic purposes. This type of exotic ssDNA–ssDNA interaction is exclusively bio-molecular in nature in the presence of Mg^{2+} and other ions present in buffer used in such study (Andersen et al. 2009; Ke et al. 2012; Rothmund 2006). Using graphene surface as template sort stranded ssDNA aggregates in spherical shapes and in elongated network (Akca et al. 2011). However, the interaction between ssDNA and single-wall carbon nano tube (CNT) constitutes DNA–carbon-nano tube hybrid (DNA–CNT) where the CNT was wrapped with a self-assembled coating of ssDNA (Johnson et al. 2010). There are several reports of fluorescing nano carbon dots to image different cell lines. Such studies are generally made use of directly using the nano carbon produced without knowing the effective amount used in those experiments (Bourlinos et al. 2008; Sun et al. 2006; Wang et al. 2010; Yang et al. 2009). The dose-related toxicity–non toxicity issue of the nano carbon used in such cell line imaging has not been addressed. Use of water-soluble carbon nano onion (wsCNO) in known amount is shown to image the entire life cycle of *Drosophila melanogaster* (Ghosh et al. 2011). In addition, the dose-dependent non-toxic and toxic use of wsCNO has also been reported in imaging the life cycle and controlling the population of mosquito, respectively (Saxena et al. 2013). In the plant system there has been a report for an optimum concentration threshold for the beneficial use of wsCNO (Saxena et al. 2014). These reports clearly suggest that there is a concentration window in the use of nano carbon and exceeding the limit it has deleterious effect to biological systems. As DNA is the most important bio-molecule that controls the structure and function of the cell, it is thus important to check the effect of wsCNO directly on dsDNA. Therefore, we

✉ Sabyasachi Sarkar
abya@iitk.ac.in; sabby@chem.iests.ac.in

¹ Department of Chemistry, Indian Institute of Technology, Kanpur, Uttar Pradesh 208016, India

² Department of Chemistry, Sister Nibedita Govt. General Degree College for Girls, Hastings House, Alipore, Kolkata, West Bengal 700027, India

³ Nano Science and Synthetic Leaf Laboratory at Downing Hall, Center for Healthcare Science and Technology, Indian Institute of Engineering Science and Technology, Shibpur, Botanic Garden, Howrah, West Bengal 711013, India

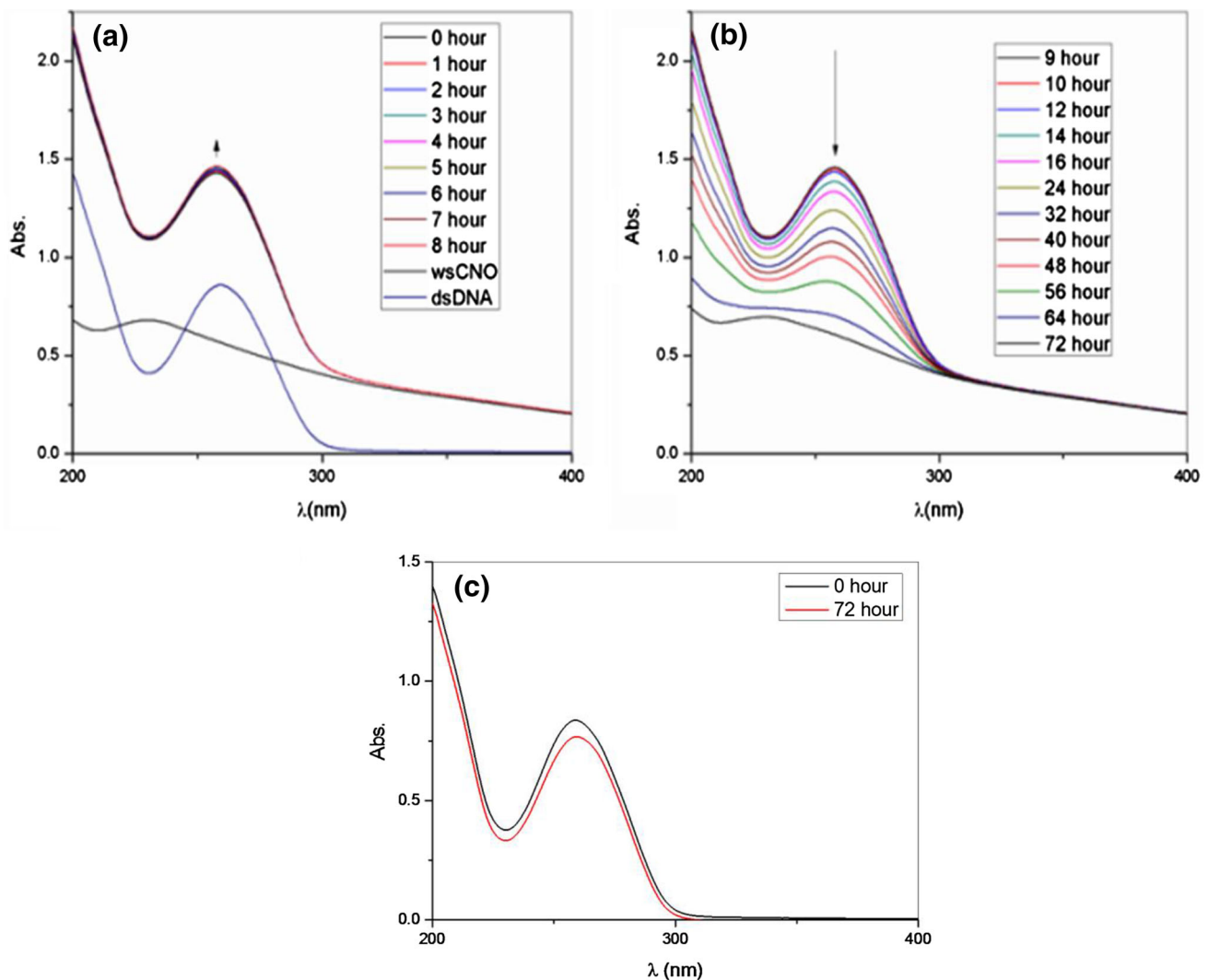


Fig. 1 **a** Time-dependent spectral change of CT-DNA with wsCNO in water in the initial period of rise in the 260 nm absorption till 8 h as labeled in the inset. *Black trace* is the electronic spectrum of wsCNO and blue trace is the electronic spectrum of CT-DNA. **b** The

gradual fall of 260 nm absorption band with time as labeled in the inset. **c** Electronic spectra of CT-DNA solution on standing for 72 h showed slight decay retaining $\sim 91\%$ of its absorption profile

report the interaction between calf-thymus (CT) dsDNA with water-soluble carbon nano onion (wsCNO) in water. We show that wsCNO first unzipped dsDNA to ssDNA and the ssDNA thus formed wrapped the wsCNO present in the solution leading to several macromolecular aggregation starting with finite shapes like triangle, polyhedron, flower petals, six-petal flowers, and finally to an extended dead-end network structure.

Experimental

Materials

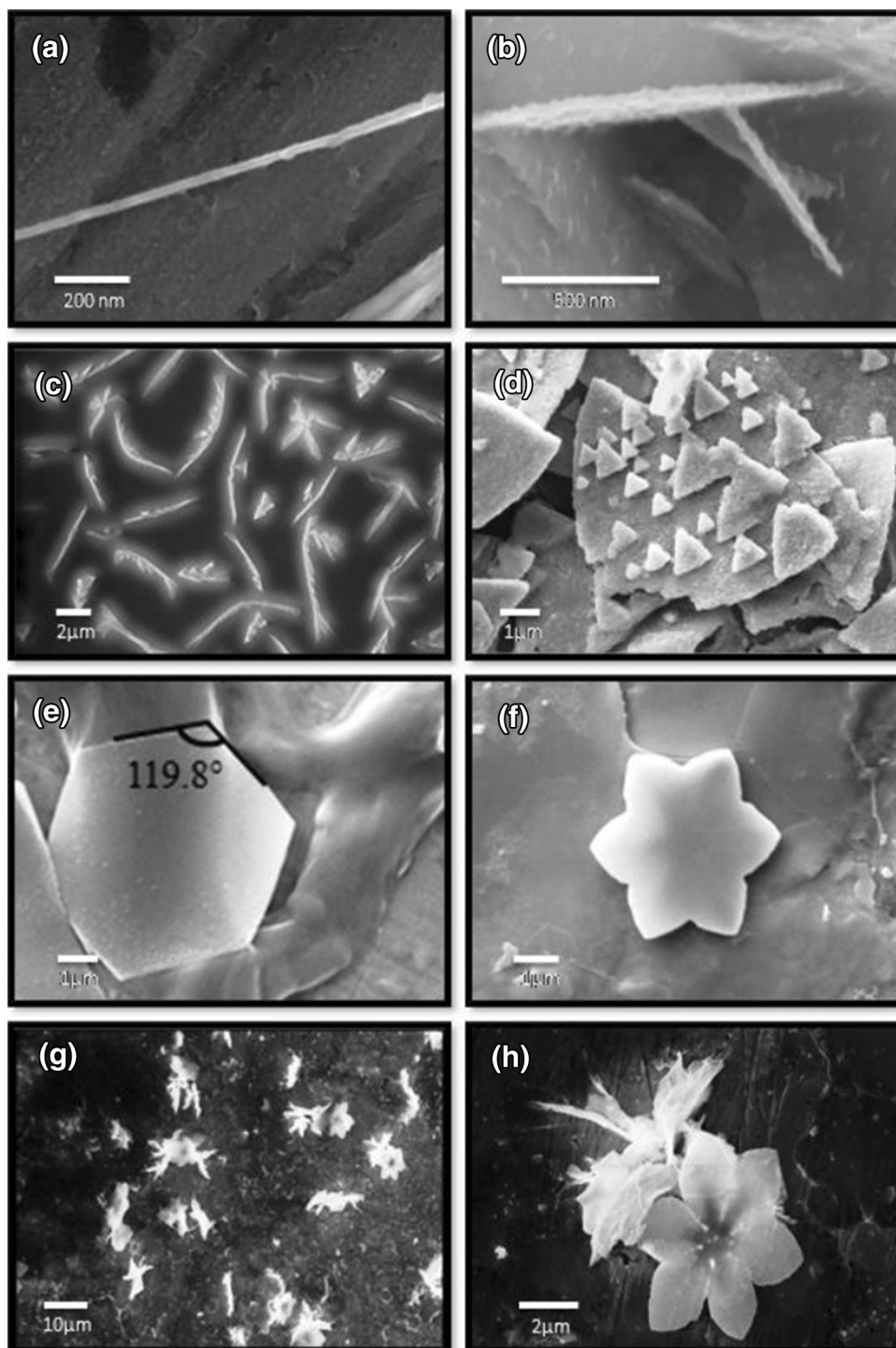
Calf thymus DNA (CT-DNA) was purchased from Sigma Aldrich (absorbance ratio $A_{260}/A_{280} = 1.8$). The water-

soluble CNOs were synthesized using previously reported methods (Ghosh et al. 2011; Sonkar et al. 2012). Water from a Millipore Milli-Q system (conductivity $\leq 0.1 \mu\text{S cm}^{-1}$) has been used.

Macroscopic and spectroscopic characterization

Electronic spectral measurements were carried out with JASCO, V-630 spectrophotometer. For optical fluorescence microscopy, slides were examined using an inverse microscope (Axiovert 200 M, Zeiss equipped with Axio Cam and AxioVision software) with FITC green filter. Solution pH were measured using Systronics Digital pH meter 335 and for scanning electron microscopy (FESEM), a SUPRA 40VP field-emission SEM (Carl Zeiss NTS GmbH, Oberkochen, Germany) equipped with an energy-

Fig. 2 Images of DNA composite; **a** 1 h: DNA-wsCNO, **b** 4 h: growth, **c** 8 h: aggregation, **d** 16 h: triangle formation, **e** hexagon, **f** flower, **g** assorted flowers, **h** selected six-petal flower



dispersive X-ray (EDX) unit, in high-vacuum mode operated at 10 kV, was used for the visualization of the size and morphology of CT-DNA-wsCNO composite.

Preparation of CT-DNA-wsCNOs composite

Calf thymus DNA (CT-DNA) (Sigma Aldrich, absorbance ratio $A_{260}/A_{280} = 1.8$) and the wsCNOs⁵ were dissolved

in water maintained at 0 °C (Millipore Milli-Q system, conductivity $\leq 0.1 \mu\text{S cm}^{-1}$). The concentration 86.66 $\mu\text{g/ml}$ of CT-DNA and 33.32 $\mu\text{g/ml}$ of wsCNO were used and when such DNA and wsCNOs solutions were mixed in 1:1 ratio, the pH of the resultant solution became 7.0. This stoichiometric ratio between CT-DNA and wsCNO is subsequently used in all experiments. The composite mixture was stored in the temperature range 1–5 °C and all

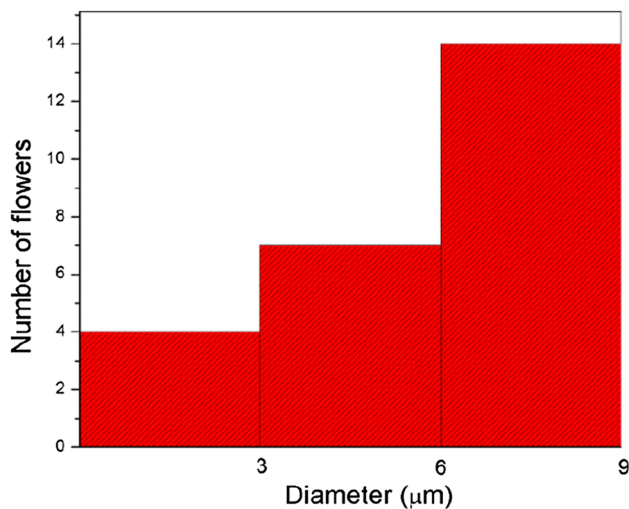


Fig. 3 Histogram: size distribution of flowers (diagonal petal–petal, data from Fig. 2g)

the experiments were carried out at a temperature of around 20 °C.

Results and discussion

As prepared the composite solution was used for successive analysis. Such a solution was first subjected to electronic spectroscopy monitoring the change in absorbance at 260 nm with time. On standing for 72 h, around a temperature in the range 1–5 °C (fridge) the solution remains clear with no precipitation as checked by centrifugation.

The hyperchromism of the CT-DNA solution reached maximum till ca 8 h (~14% increase) and then its intensity gradually started decreasing. After 64 h most of the intensity measured at 260 nm absorption band is lost and after 72 h it completely disappeared. The spectral trace after 72 h clearly retains the absorption signature of wsCNO at 230 nm which was masked under the strong back ground absorption of DNA at the earlier stages of the mixture. Around 9% degradation of CT-DNA was monitored by following the decrease in the intensity of 260 nm band under controlled conditions after 72 h (Fig. 1c). The complete loss of this characteristic absorption on the addition of wsCNO in this time frame suggests that wsCNO completely damage DNA initiating its aggregation leading to unnatural chain aggregates. The rise in the intensity of the absorption band at 260 nm of CT-DNA (dsDNA) in the presence of wsCNO in the initial period is related to its denaturation to ss-DNA. It is known that the electronic absorption profile of ssDNA is identical to that of dsDNA with the variation in increase in the intensity of absorption (Berg et al. 2002; Wang and Son 2013). When the bases of dsDNA got completely un-stacked, the

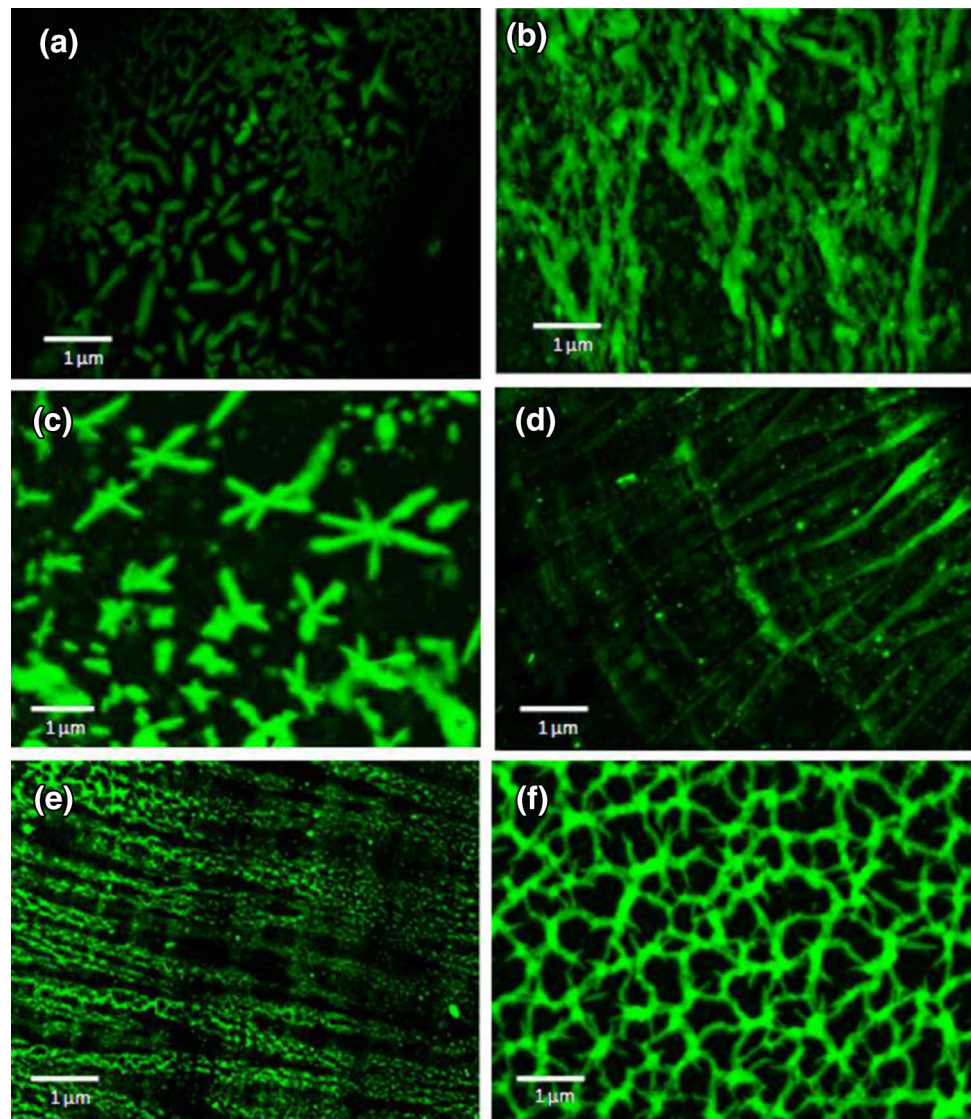
wavelength of maximum absorbance at 260 nm does not change but for the total conversion from dsDNA to ssDNA the absorption increases by 37% (Berg et al. 2002). However, under wsCNO only 14% increase of this intensity at the initial phase is noticed and this intensity remained constant in the initial time period between 4 and 8 h. Therefore, in the present case it is around 38% denaturation of dsDNA to ssDNA that can be monitored and this concentration remained unchanged for 8 h. We interpret this phenomenon as the spherical wsCNO possessing several carboxylic and hydroxyl groups initially interacting to unzip the CT-DNA (dsDNA) to ssDNA. Once this process sets in, a follow-up reaction by the separated ssDNA started to wrap the wsCNO using hydrogen bond and other conventional forces. Such interactions may cause significant structural changes of ssDNA with the loss in its characteristic absorption at 260 nm. Once the speed in wrapping exceeded the denaturation of ds-DNA to ssDNA the characteristic DNA absorption peak at 260 nm continuously loses its intensity as monitored in the subsequent time-dependent absorption spectra (Fig. 1b). The denaturation rate from dsDNA to ssDNA may be slower than its wrapping by wsCNO kinetics which apparently prevents to display further increase in the intensity of the 260 nm peak at a later stage. The time-dependent response of the electronic spectra is shown in Fig. 1. Figure 1a shows the initial rise in the absorption of DNA due the denaturation of dsDNA to ssDNA. However, after the initial build up of 38% ssDNA within 8 h it started to react more rapidly with wsCNO as shown by the time-dependent subsequent electronic spectral scan from 9 to 72 h (Fig. 1b). The scan after 72 h showed the complete disappearance of the signature band at 260 nm associated with DNA. Under identical conditions the stability of CT DNA was measured as control to show that only ~9% of its intensity is lost retaining 91% DNA intact (Fig. 1c).

SEM and fluorescence optical microscopy

Based on the electronic spectral time frame we imaged the mixture of CT-DNA and wsCNO by SEM and also by fluorescence optical microscopy to understand the nature of such interaction visually.

The hydrophilic groups like –COOH and –OH attached to the outer shell of wsCNOs may interact directly with unzipped ssDNA and may also help to unzip dsDNA competing with hydrogen bonding and/or van der Waals interaction. The SEM images of sample mixture are shown from the initial mixing till 16 h in Fig. 2. In the beginning (Fig. 2a) the image may relate to a dsDNA with surface interaction of wsCNO. After 4 h (Fig. 2b) the aggregation at several places were observed and between 8 and 16 h such interaction clearly developed branched and designed

Fig. 4 Fluorescence microscopy images with time: **a** 1 h, **b** 4 h, **c** 16 h, **d** 24 h, **e** 48 h, **f** 72 h



structure aggregation (Fig 2c, d). Fig. 2e–h shows the aggregation pattern where Fig. 2h is a zoomed image of a six-petal structure similar to a flower. At this point the absorption of DNA at 260 nm started to lose its intensity suggesting the loss of known structure of DNA. Figure 2d shows the predominant shape of the composite like triangle after 16 h. These triangles aggregate to create hexagon (angle of 119.8°) as shown in Fig. 2e. Peripheral attachment of these triangles to a hexagon may lead to six-petal design of flower as in Fig. 2f. Figure 2g shows assorted sizes of such flower-shape structure. A histogram (Fig. 3) shows the size distribution pattern of such structures where large flowers with diagonal petal–petal distribution of $9 \mu\text{m}$ are observed. A representative six-petal shaped flower esthetically pleasing like natural flower is shown in

Fig. 2h. The association of fluorescing wsCNO in such aggregation process is followed by imaging the mixture with the progress in reaction time. Figure 4 displays the fluorescence images of the composite in different time intervals. In the beginning hour (Fig. 4a), the aggregation started and became extensive during 4 h (Fig. 4b). At 16 h the different shapes with the aggregation like six-petal flowers are visible (Fig. 4c). The interesting part here is to image the aggregate in the next 24, 48 and 72 h, respectively. Figure 4d–f clearly shows the progress in aggregation that ended with dead-end extended network structure. It is to be noted that the time period for such aggregation using SEM or fluorescence study is around 16 h. The electronic spectral study shows the DNA signature till 64 h with very low intensity This suggests that the SEM matrix

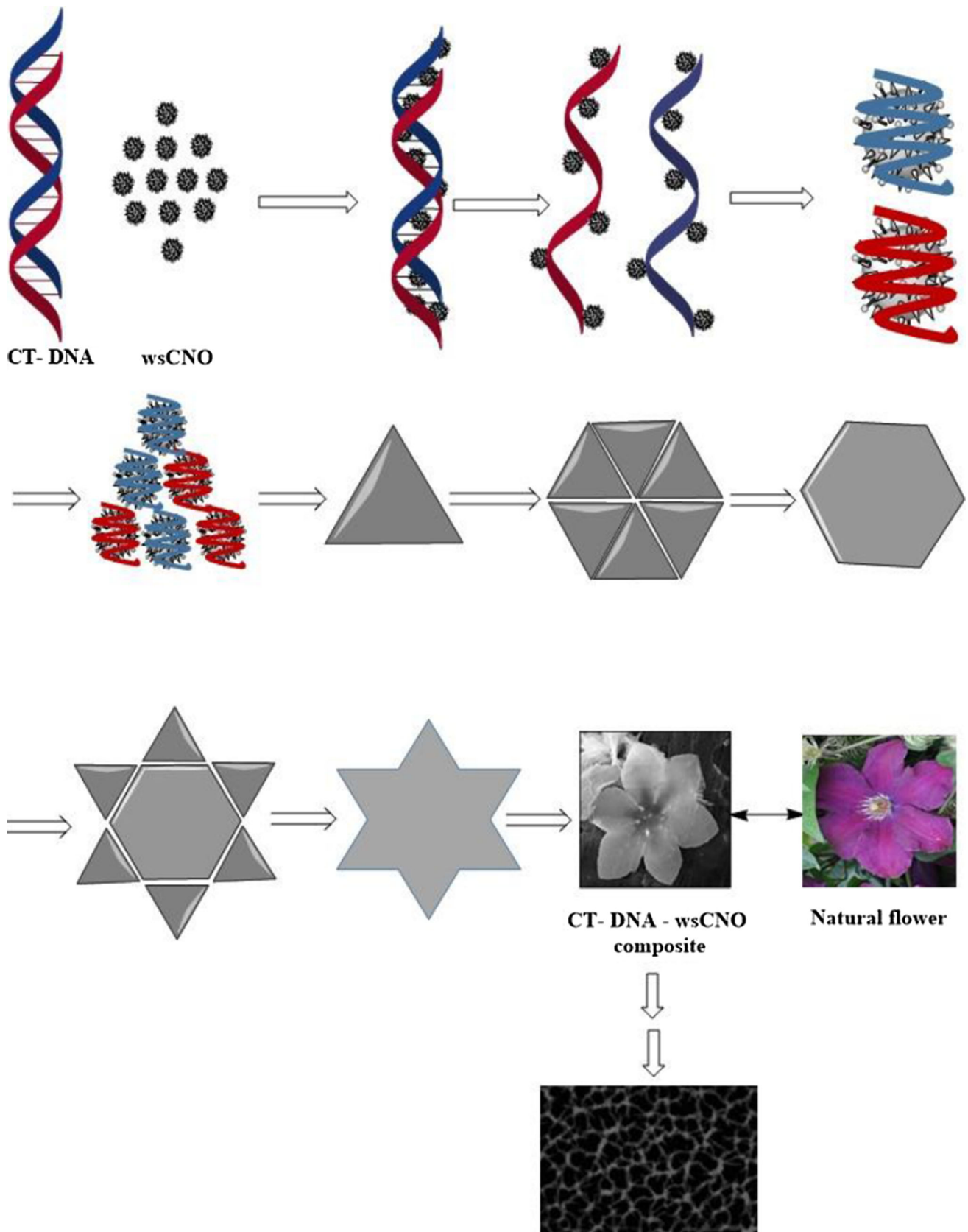


Fig. 5 The formation of flower shape composite of wsCNOs and CT-DNA with triangle and hexagon as intermediates finally to dead-end network structure

or the microscopic slide may accelerate aggregation, especially when the water gets dried up with time (Mitra and Sarkar 2016). The possible process from denaturation to petal shape followed with the flower type growth formation is schematically shown in Fig. 5. The spontaneous formation of triangle-shaped aggregate at the initial stage may be due to the shape-related thermodynamic drive to acquire stability which further led to create stable hexagon structure.

Conclusion

In conclusion, wsCNOs is shown to unzip CT-DNA in water to ssDNA. Once appreciable ssDNA is available, the spherical wsCNO spontaneously wraps ssDNA by its peripheral carboxylic acid and hydroxyl groups used as spikes. The assembly of this wrapped species leads to the formation of triangle, hexagon and flower shapes with several micrometers in sizes. Finally, at the end these regular structures may be driven to more stable network structure with the creation of extended dead-end network structure losing normal characteristics of DNA. As wsCNO is shown to be dose-dependent non-toxic (Ghosh et al. 2011; Saxena et al. 2013, 2014) it will be challenging to explore the interaction of wsCNO with rouged DNA to control their unwanted proliferation in certain cell growth and preventing such viral DNA replication in well-known diseases.

Acknowledgements DB and BP acknowledge CSIR, New Delhi, India for Senior Research Fellowships. SS thanks SERB-DST(SR/S1/RFIC-01/2011 and EMR/2015/001328), New Delhi, India for sustained financial support.

Open Access This article is distributed under the terms of the Creative Commons Attribution 4.0 International License (<http://creativecommons.org/licenses/by/4.0/>), which permits unrestricted use, distribution, and reproduction in any medium, provided you give appropriate credit to the original author(s) and the source, provide a link to the Creative Commons license, and indicate if changes were made.

References

- Akca S, Foroughi A, Frochtzvajg D, Postma HWC (2011) Competing interactions in DNA assembly on graphene. *PLoS One* 6:e18442. doi:10.1371/journal.pone.0018442
- Andersen ES et al (2009) Self-assembly of a nanoscale DNA box with a controllable lid. *Nature* 459:73–76. doi:10.1038/nature07971
- Berg JM, Tymoczko JL, Stryer L (2002) *Biochemistry*, 5th edn. W. H. Freeman and Company, New York
- Bourlinos AB, Stassinopoulos A, Anglos D, Zboril R, Georgakilas V, Giannelis EP (2008) Photoluminescent carbonogenic dots. *Chem Mater* 20:4539–4541. doi:10.1021/cm800506r
- Ghosh M, Sonkar SK, Saxena M, Sarkar S (2011) Carbon nano-onions for imaging the life cycle of drosophila melanogaster. *Small* 7:3170–3177. doi:10.1002/sml.201101158
- Johnson RR, Johnson ATC, Klein ML (2010) The nature of DNA-base-carbon-nanotube interactions. *Small* 6:31–34. doi:10.1002/sml.200901481
- Ke Y, Voigt NV, Gothelf KV, Shih WM (2012) Multilayer DNA origami packed on hexagonal and hybrid lattices. *J Am Chem Soc* 134:1770–1774. doi:10.1021/ja209719k
- Mitra J, Sarkar S (2016) Substrate induced morphology in a hydrosulfide-molybdenum complex. *New J Chem* 40:8905–8910. doi:10.1039/C6NJ01910B
- Rothmund PWK (2006) Folding DNA to create nanoscale shapes and patterns. *Nature* 440:297–302. doi:10.1038/nature04586
- Saxena M, Sonkar SK, Sarkar S (2013) Water soluble nanocarbons arrest the growth of mosquitoes. *RSC Adv* 3:22504–22508. doi:10.1039/C3RA44100H
- Saxena M, Maity S, Sarkar S (2014) Carbon nanoparticles in ‘biochar’ boost wheat (*Triticum aestivum*) plant growth. *RSC Adv* 4:39948–39954. doi:10.1039/C4RA06535B
- Sonkar SK, Roy M, Babar DG, Sarkar S (2012) Water soluble carbon nano-onions from wood wool as growth promoters for gram plants. *Nanoscale* 4:7670–7675. doi:10.1039/C2NR32408C
- Sun Y-P et al (2006) Quantum-sized carbon dots for bright and colorful photoluminescence. *J Am Chem Soc* 128:7756–7757. doi:10.1021/ja062677d
- Wang X, Son A (2013) Effects of pretreatment on the denaturation and fragmentation of genomic DNA for DNA hybridization. *Environ Sci Process Impacts* 15:2204–2212. doi:10.1039/C3EM00457K
- Wang X et al (2010) Bandgap-like strong fluorescence in functionalized carbon nanoparticles. *Angewandte Chemie Int Ed* 49:5310–5314. doi:10.1002/anie.201000982
- Yang S-T et al (2009) Carbon dots for optical imaging in vivo. *J Am Chem Soc* 131:11308–11309. doi:10.1021/ja904843x